EUROfusion

EUROFUSION CP(15)04/06

A. De Backer et al.

Primary Damage in Tungsten Using the Binary Collision Approximation, Molecular Dynamic Simulations and the Density Functional Theory

(18th May 2015 – 22nd May 2015)
Aix-en-Provence, France

This work has been carried out within the framework of the EUROfusion Consortium and has received funding from the Euratom research and training programme 2014-2018 under grant agreement No 633053. The views and opinions expressed herein do not necessarily reflect those of the European Commission.

Primary damage in tungsten using the Binary Collision Approximation, Molecular Dynamic simulations and the Density Functional Theory

A. De Backer[1,*], A. Sand[2], C.J. Ortiz[3], C. Domain[4], P. Olsson[5], E. Berthod[6], C.S. Becquart[6]

[1] *CCFE, Culham Centre for fusion Energy, Abingdon, Oxon OX14 3DB, United Kingdom*

[2] *Department of Physics, University of Helsinki, P.O. Box 43, FI-00014, Helsinki, Finland*

[3] *Laboratorio Nacional de Fusión por Confinamiento Magnético, Av. Complutense 40, Madrid, Spain*

[4] *EDF Lab Les Renardieres, Dpt MMC, 77250 Moret sur Loing, France*

[5] *KTH Royal Institute of Technology, Reactor Physics, Roslagstullsbacken 21, 10691 Stockholm, Sweden*

[6] *UMET, UMR 8207, Université Lille I, 59655 Villeneuve d'Ascq cédex, France*

Abstract

The damage produced by primary knock-on atoms (PKA) in W has been investigated from the threshold displacement energy (TDE) where it produces one Self Interstitial Atom (SIA) – vacancy pair to higher energies, up to 100 keV, where a large melted zone is formed. The TDE has been determined in different crystal directions using the Born Oppenheimer Density Functional Molecular Dynamics (DFT-MD). A significant difference has been observed without and with the semi-core electrons in particular in the ⟨111⟩ direction where we found respectively 44 eV and more than 80 eV. Classical MD (MD) has been used with two different empirical potentials characterized as "soft" and "hard" to obtain statistics on TDEs. Cascades at higher energy have been calculated, with these potentials, using the code PARCAS and a model that accounts for electronic losses [1]. Two other sets of cascades have been produced using the Binary Collision Approximation (BCA): a Monte Carlo BCA using SDTrimSP [2] (similar to SRIM [3]) and MARLOWE [4]. To account for the recombination of defects happening during the thermal spike, we used a recombination distance determined comparing the distributions of SIA-vacancy pairs as a function of their mutual distance in SDTrimSP and MD cascades. We found the most appropriate value for the recombination distance to be 12 Å, a larger value than the one we determined using MARLOWE in a previous work [5]. This comes from the fact

**Corresponding author E-mail: andree.debacker@ccfe.ac.uk*

that in this work we investigate cascades in the bulk whereas surface cascades, which are known to produce much more defects [6,7], were modelled in [5]. Finally, another significant difference between BCA and MD cascades is the clustering of SIAs and vacancies. Preliminary results showed that this difference is considerably reduced after annealing the cascade debris at 473 K using our Object Kinetic Monte Carlo model, LAKIMOCA [8].

1- Introduction

The evaluation of the damage produced by ions or neutrons usually uses models based on the Binary Collision Approximation (BCA) or on Molecular Dynamics (MD) simulations. BCA based models are faster but require parameters such as threshold displacement energies or recombination radius. Full MD cascades are computer time consuming and rely on the development of empirical potentials. Furthermore, the damage evolves with time and temperature on multiple scales because of the mobility of the defects and their interactions and different techniques must be used to model it. Given the short length of this paper we briefly describe the methods we have used prior to the result description. In the first section we present some results about the threshold displacement energies obtained by DFT-MD and classic MD. The second section concerns the recombination distance that we determined by comparing BCA to MD cascades. In the last part, the defect cluster formation is briefly analyzed and preliminary results on the annealing of cascades using an OKMC are discussed.

2- Threshold displacement energies

DFT-MD simulations in the Born-Oppenheimer approximation have been performed over a large range of angles and knock-on energies in the micro-canonical (NVE) ensemble. The projector augmented wave (PAW) formalism [9,10] has been applied in the generalized gradient approximation [11]. These methods are implemented in the Vienna Ab initio Simulation Package (VASP) [12]. Non-cubic supercells of at least 648 bcc sites (9×6×6) have been used for the dynamic simulations. The DFT calculations were performed using two kinds of potentials: the minimal set regular PAW which

*Corresponding author E-mail: andree.debacker@ccfe.ac.uk

considers 6s and 5d electrons as valence electrons and the semi-core PAW which also considers the 5p electrons. The minimal set regular projector augmented-wave (PAW) will be referred to as DFT, whereas the semi-core PAW will be referred to as DFT-sc. The time step used in the DFT-MD simulations was set from 1.5 to 3 fs depending on the PKA energy, after some tests were performed. All results here presented were obtained using the gamma point in the Brillouin zone and a cut-off of 230 eV.

As in our previous work in iron [13], to calculate TDEs, one initiates a collision sequence along a specific direction, by giving the PKA, a kinetic energy, and more precisely a velocity along the direction chosen at 0 K. If at the end of the collision cascade no defect remains in the lattice, the PKA velocity is increased and a new simulation is launched. The TDE is the minimum at which a FP is observed at the end of the simulation.

For MD runs, one of Marinica et al potentials [14] has been interpolated to ZBL potential [15] in two different ways. They have been characterized as “soft” (MS-s) and “hard” (MS-h). For more statistics, 7000 MD runs were done in 12×12×16 atom boxes as in [16], after 6 ps of thermalisation at 36 K. From one run to another, the initial condition varies by the selection of the PKA among the 8 atoms in the middle of the simulation box and the Miller indexes of the exact lattice direction which are incrementally changed by 0.2.

Table 1 gives the TDEs obtained by DFT-MD and MD methods. “DFT” and “DFT-sc” conditions gave DTE equal respectively to 40 eV and 58 eV in the ⟨100⟩ direction. Results in ⟨110⟩ and ⟨111⟩ directions are higher. MD results are usually smaller than DFT and exhibit a broad distribution illustrated Figure 1a. As expected from its “hard” character, MS-h predicts a higher TDE than MS-s and DFT-sc, a higher threshold energy than DFT. Another way of comparing these four cohesive models is by calculating the evolution of the energy increase when the initial atom is moved toward its nearest neighbour in a rigid lattice. This will be referred to as Quasi Static Drag (QSD). QSD energy is showed

*Corresponding author E-mail: andree.debacker@ccfe.ac.uk

for the ⟨100⟩ direction on Figure 1b. It appears clearly that the two conditions that predict higher energy threshold, i.e. DFT-sc and MS-h, exhibit a significantly higher QSD energy for distance ranging from 1 to 1.5 Å. The pair energy predicted by the ZBL potential is also reproduced which illustrates the difference in the interpolation of both empirical potentials. The DFT-sc condition is the quite close to the ZBL potential. At equilibrium, the first nearest neighbour in the ⟨100⟩ direction is at 3.17 Å but during an MD simulation, an atom with high kinetic energy may come closer than 1.5 Å to its first nearest neighbour and the difference behaviour of the potentials at short distances will have an impact on the energy transfer and the probability of a FP formation and finally the resulting TDE. The TDEs correlate with the QSD energy when two atoms are separated by a distance of 1 – 2 Å: in DFT-MD and MD, the larger the energy, the larger the TDE.

Table 1. Threshold Displacement Energies for the different cohesive models along different crystal orientation.

in eV	DFT	DFT-sc	MS-s	MS-h
⟨100⟩	40	58	31	43
⟨110⟩	63	>80	51	71
⟨111⟩	44	>80	45	65

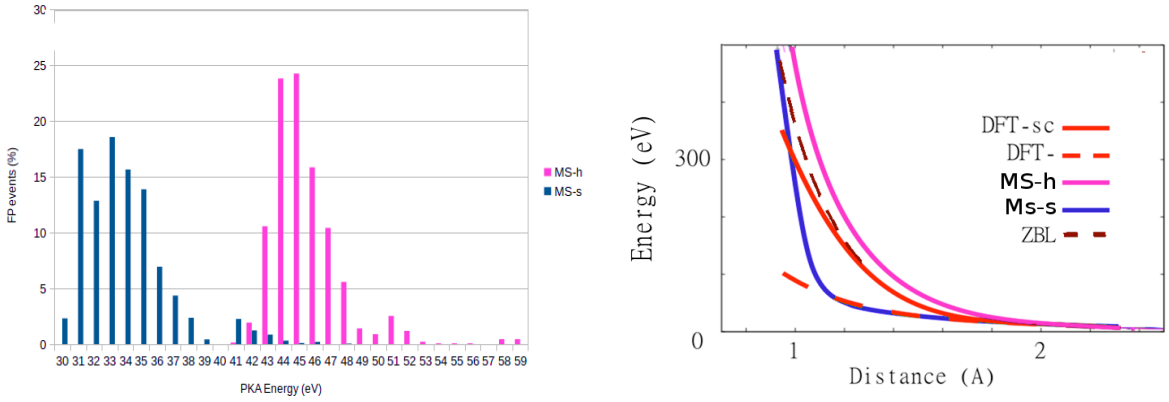

Fig. 1. (a) Statistic of FP formed as a function of the PKA energy in MD runs using the MS-h (hard) and MS-s (soft) empirical potentials; (b) Energy increase when one atom is displaced toward its

*Corresponding author E-mail: andree.debacker@ccfe.ac.uk

first nearest neighbour *in the* ⟨100⟩ *direction with the different cohesive models.*

3- The recombination distance

In this work, BCA and full classical MD cascades have been calculated for the same PKA energies, both models accounting for electronic losses. BCA computes the development of cascade trajectories triggered by an energetic atom as a sequence of binary collisions rather than integrating the equations of motion of the whole system over time, as would be done with full MD.

The BCA has been combined with a Monte Carlo approach to model the cascade formation in slightly different models in SRIM [3] and SDTrimSP [2]. We used SDTrimSP whose model is fully detailed in [17]. The DTE, binding energy and cutoff energy are the main parameters of this model. In a first attempt, we used the concept of the DTE with an average value of 51 eV. In this approach, if the moving atom, which can be the initial projectile or one of the recoils, and the collided atom have a kinetic energy higher than the TDE, after the collision, a stable vacancy is considered to be formed. If both atoms stay with a kinetic energy lower than the DTE, a Self Interstitial Atom (SIA) is formed. If only the kinetic energy of the impinging atom is lower than the threshold energy, a replacement collision occurs and in the opposite case the collision causes no defect.

Full cascade simulations were performed using PARCAS and MS-s and MS-h potentials for PKAs ranging from 1 to 100 keV. The simulations were performed at 0 K with periodic boundary conditions and random PKA directions. A Berendsen thermostat was applied to border atoms, to allow for heat transfer out of the cell, and to inhibit cascade self-interaction. Electronic stopping was included through the use of a friction term, applied to all atoms with kinetic energy above 10 eV [1]. To analyze the MD cascades, a Wigner-Seitz (WS) analysis was done. The lattice is divided into WS cells and when one WS is empty, the coordinate of the cell is given as a vacant site.

The number of vacant sites as a function of time can be compared on Figure 2a for 20 keV BCA and

*Corresponding author E-mail: andree.debacker@ccfe.ac.uk

MD cascades. The calculations exhibit a similar evolution up to 100 fs. After that time, a plateau is reached in the BCA whereas full classical MD predicts a two to three times higher maximum at 300 – 500 fs. The BCA simulations do not count for any recombination of vacancies and interstitials and with the threshold energy of 51 eV, it was not possible to reproduce the MD results (maximum number and final number of defects). It can be noticed that the softer potential predicted more vacant sites at the maximum. The cause is the lower energy transfer to surrounding atoms which has two effects: 1) there are less "vacancies" at peak damage because there is less of a heat spike, and 2) the weaker heat spike means less recombination at the later phase, resulting in more surviving defects. Also, since there is less energy transfer to surrounding atoms, the recoils themselves can travel further, which results in less in-cascade recombination.

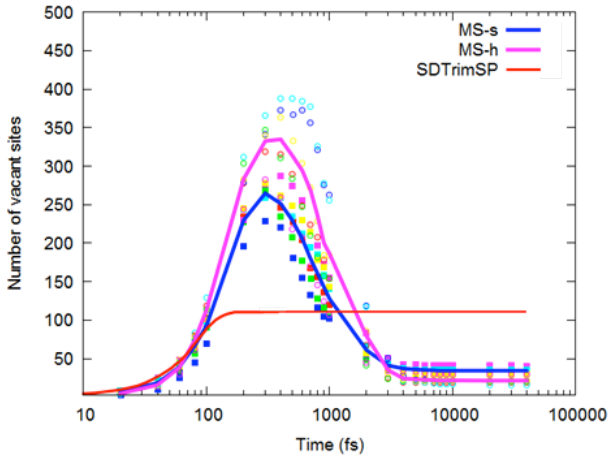

Fig. 2. (a) Number of vacant sites in 20 keV full classical MD and BCA cascades as a function of time.

We then used the concept of recombination distance as we did with MARLOWE [4,5,18]. MARLOWE is based on the BCA and takes into account the crystalline structure of materials, which allows accounting for crystal lattice effects such as channeling and focusing chains that may influence trajectories and subsequent atomic displacements. An atom is displaced from its lattice site if the projectile transfers during the collision energy higher than its binding energy to the crystal. In the case of metals, the binding energy of a lattice atom corresponds to the cohesive energy. As SDTtrimSP, MARLOWE does not account for long-range interactions between defects and cannot hence account

*Corresponding author E-mail: andree.debacker@ccfe.ac.uk

for the recombination of SIAs and vacancies during the cascade. However, it is possible to emulate the spontaneous recombination of SIA and vacancies that occurs during the thermal spike regime by considering a spherical volume capture between the defects. Cascades obtained with MARLOWE were calculated using the ZBL potential [1] in the ⟨111⟩ direction for PKA energies of 1, 20, 100 and 400 keV. The binding energy was taken equal to 8.9 eV and the recombination distance was 1.2 a_0, where a_0 is tungsten lattice parameter.

With SDTrimSP, we mimicked this method by equaling the DTE to the binding energy. Many more defects are formed, in particular close defects, which do not exist in full classical MD cascades. After the cascade calculation, the vacancies and SIA are paired starting with the ones which are closest from each other and eliminated when they are less distant that the recombination distance. The recombination distance should be a unique value that leads to similar number of defects in BCA and MD cascades but both potential (MS-s) predicted different defect number. The soft potential gave in particular more SIA-vacancy pairs of small mutual distance. Furthermore to reproduce the full energy range MD results, two significantly different recombination radii need to be used. For the 1 keV cascades, a recombination radius equal to 4.5 Å which is close to the one we obtained in [5] provides agreement between MD and BCA, whereas for the higher energy cascades a much larger recombination radius close to 12 Å was necessary. The distributions of SIA-vacancy pairs as a function of their mutual distance in BCA and MD (with MS-s) cascades are plotted on Figure 3a. When the recombination distance is used the small distance part of the distribution is truncated however a deficit of small pairs and large pairs (70 – 200 Å) remains as well as an excess in between, compared to MD cascades.

Figure 3b shows the number of pairs of defect as a function of the PKA energy predicted by the different models. As expected BCA models without the recombination distance overestimate this number and SDTrimSP with the recombination distance is close to MD. However MARLOWE, used

*Corresponding author E-mail: andree.debacker@ccfe.ac.uk

with a recombination distance equal to 3.8 Å predicts 5 – 10 times more defects than MD. The discrepancy between the recombination distance obtained in our previous work and the one found here comes from the fact that here cascades have been simulated in the bulk whereas it was surface cascades in our previous work [5]. In [6] a factor 2 between defects in cascades on surface and in bulk is reported.

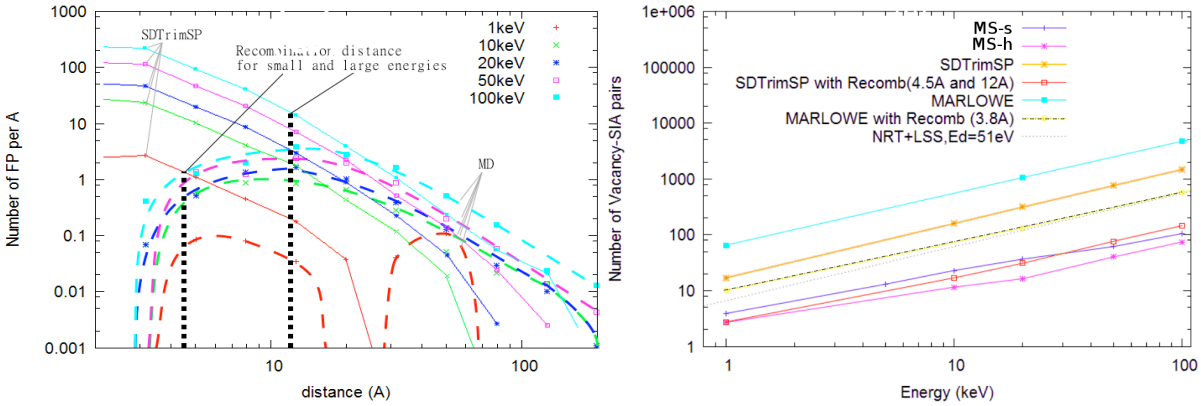

Fig. 3. (a) Average distributions of SIA-vacancy pairs as a function of their mutual distance in SDTrimSP and full MD cascades with MS-s potential, for PKA energies ranging from 1 keV to 100 keV; (b) number of pairs of defects as a function of the PKA energy predicted by all the models with used.

Visual inspection of final cascades produced by the different methods is instructive and pictures of 100 keV are reproduced on Figure 4. SDTrimSP produces cascades where the vacancies are generally concentrated inside the damaged zone while SIAs are found mainly around. In the MARLOWE cascades, remains of long replacement sequences along ⟨111⟩ directions are visible. MD cascades contain fewer defects and several MS-h cascades contain one large SIA loop while the MS-s shows smaller clusters.

*Corresponding author E-mail: andree.debacker@ccfe.ac.uk

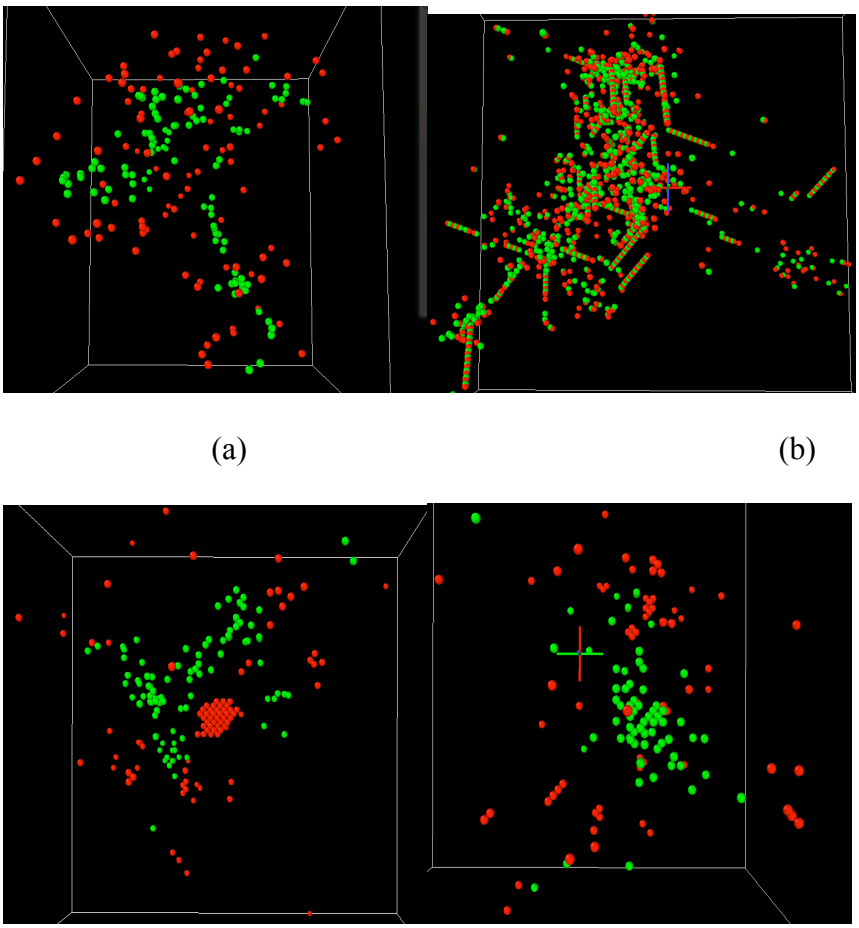

Fig. 4. Pictures of 100 keV cascades using (a) SDTrimpSP + recomb, (b) Marlowe + recomb, (c) MD with MS-h and (d) MD with MS-s. Vacancies are in green and SIA in red.

Annealing of individual cascades have been done with our OKMC code, LAKIMOCA [8] using the parameterization described in [19] at 473 K. We report here the statistic coming from annealing of each individual cascades in a 200×200×200 simulation box. In the distribution of vacancy and SIA clusters showed Figures 5, the defects present in the box are summed to the ones that reach the surface of the box. This procedure gives the concentrations of defects as a function of their size that result from the intra-cascade interactions. It could be considered later as the source term for larger scale models such as the mean field Rate Theory [20]. It is visible that SIA clusters are present in the MD cascades from

*Corresponding author E-mail: andree.debacker@ccfe.ac.uk

the beginning and are much larger with the MS-h potential. During the annealing, the clusters grew significantly by accumulation of diffusing single SIAs. SIA clusters which were not present initially in SDTrimSP cascades formed during the annealing and their distribution follows a similar tendency. However, the sizes obtained never compare to the largest clusters of the MD cascades. The difference in the SIA cluster size distribution between MD and SDTrimSP is visibly reduced at the end of the annealing. At the investigated temperature, vacancies do not diffuse in W. During the annealing vacancy clusters mainly shrink by recombination with SIAs. A very small amount of vacancy clusters are reported in BCA cascades because of their concentration at the centered of the damaged zone and further statistics are necessary to determine if the difference between MD and BCA is similar to the difference between MD cascades with the different potentials.

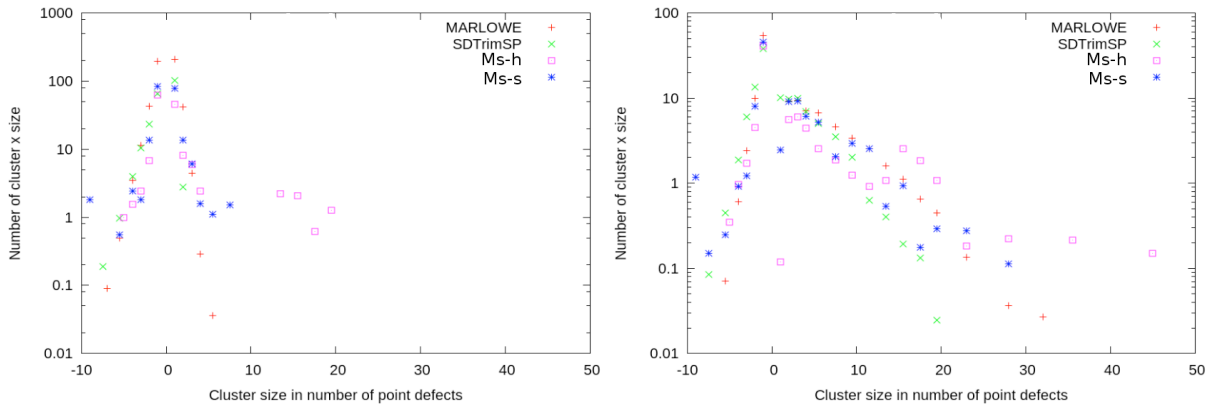

Fig. 5. Averaged distributions of defect clusters (vacancy, resp. SIA, clusters are the negative, resp. positive, part of the plot) after 0 s (a) and 10^{-6} s (b) of annealing of 100 keV cascades obtained with the different cohesive models, at 473 K using our OKMC model, LAKIMOCA.

4- Conclusion

This work illustrates how a multiscale approach reveals some key aspects in the modeling of the damage produced by irradiation. Work is in progress to further analyse the quality of empirical

*Corresponding author E-mail: andree.debacker@ccfe.ac.uk

potential and link atomistic properties and defects produced in cascades. The OKMC model should be used along with other techniques such as Mean Field Rate theory to investigate the long term evolution at several temperatures which would allow comparison with experimental results.

Acknowledgement

This work was part-funded by the RCUK Energy Programme [grant number EP/I501045] and the European Union's Horizon 2020 research and innovation programme. This work is supported by CEA under the collaborative contract number V 3542.001 on Fusion engineering issues. This research has been done using the CRI supercomputer of the Université Lille1 – Sciences et Technologies supported by the Fonds Européens de Développement Régional. This work contributed to the Enabling Research project on tritium retention in controlled and evolving microstructure.

References

[1] A. E. Sand, S. L. Dudarev and K. Nordlund, EPL, 103 (2013) 46003.

[2] W. Eckstein A. Mutzke, R. Schneider, R. Dohmen, "SDTrimSP: Version 5.00." IPP, Report 12/8, (2011).

[3] www.srim.org

[4] RSICC Home Page. https://rsicc.ornl.gov/codes/psr/psr1/psr-137.html (accessed May, 2014).

[5] M. Hou, C. J. Ortiz, C.S. Becquart, C. Domain, U. Sarkar, A. De Backer, J. Nucl. Mater., 403 (2010) 89.

[6] R. E. Stoller, J. Nucl. Mater., 307 (2002) 935.

[7] K. Nordlund, J. Keinonen, M. Ghaly, R. S. Averback, Nature, 398 (1999) 49.

[8] C. Domain, C.S. Becquart, L. Malerba, J. Nucl. Mater., 335 (2004) 121.

[9] P. E. Blöchl, Phys. Rev. B 50, (1994) 17953.

[10] G. Kresse and D. Joubert, Phys. Rev. B 59, (1999) 1758.

**Corresponding author E-mail: andree.debacker@ccfe.ac.uk*

[11] J. P. Perdew, et al., Phys. Rev. B 46, (1992) 6671.

[12] G. Kresse and J. Hafner, Phys. Rev. B 47 (1993) 558; ibid. Phys. Rev. B 49, (1994) 14251; G. Kresse and J. Furthmüller, Comput. Mat. Sci., 6 (1996) 15; ibid. Phys. Rev. B, 54 (1996) 11169.

[13] P. Olsson, C. Domain, Proc. Int. Conf. Multiscale Mater. Model., 5th, Freiburg, Ger, (2010) 4.

[14] M.-C. Marinica et al., "J. Phys. Condens. Matter, 25, 39 (2013) 395502.

[15] J.F. Ziegler, J.P. Biersack, U. Littmark, Pergamon, New York, 1985; www.srim.org

[16] K. Nordlund, J. Wallenius, et L. Malerba, Nuclear Instruments and Methods in Physics Research, 246 (2006) 322.

[17] W. Eckstein, "Computer Simulation of Ion-Solid Interactions," Springer Series in Materials Science, vol 1 (1991).

[18] C. J. Ortiz, A. Souidi, C.S. Becquart, C. Domain, M. Hou, Radiation Effects and Defects in Solids 169 (2014) 592.

[19] C. S. Becquart, C. Domain, U. Sarkar, A. De Backer, M. Hou, J. Nucl. Mater., 403 (2010) 75.

[20] T. Jourdan and J.-P. Crocombette, Phys. Rev. B, 86 (2013) 054113.

Corresponding author E-mail: andree.debacker@ccfe.ac.uk